Published in final edited form as:

Anal Chem. 2023 May 09; 95(18): 7178–7185. doi:10.1021/acs.analchem.2c05616.

Membrane protein binding interactions studied in live cells via diethylpyrocarbonate covalent labeling-mass spectrometry

Zachary J. Kirsch[1], **Jeanna M. Blake**[2], **Uyen Huynh**[1], **Dheeraj K. Agrohia**[1], **Catherine Y. Tremblay**[1], **Eric M. Graban**[2], **Robert C. Vaughan**[2], **Richard W. Vachet**[1,*]

[1]Department of Chemistry, University of Massachusetts, Amherst, Massachusetts 01003, United States

[2]QuarryBio, Collins Building, 2051 East Paul Dirac Dr., Tallahassee, FL 32310

Abstract

Membrane proteins are vital in the human proteome for their cellular functions and make up a majority of drug targets in the US. However, characterizing their higher-order structures and interactions remains challenging. Most often membrane proteins are studied in artificial membranes, but such artificial systems do not fully account for the diversity of components present in cell membranes. In this study, we demonstrate that diethylpyrocarbonate (DEPC) covalent labeling-mass spectrometry can provide binding site information for membrane proteins in living cells using membrane-bound tumor necrosis factor α (mTNFα) as a model system. Using three therapeutic monoclonal antibodies that bind TNFα, our results show that residues that are buried in the epitope upon antibody binding generally decrease in DEPC labeling extent. Additionally, serine, threonine, and tyrosine residues on the periphery of the epitope increase in labeling upon antibody binding because of a more hydrophobic microenvironment that is created. We also observe changes in labeling away from the epitope, indicating changes to the packing of the mTNFα homotrimer, compaction of the mTNFα trimer against the cell membrane, and/or previously uncharacterized allosteric changes upon antibody binding. Overall, DEPC-based covalent labeling-mass spectrometry offers an effective means of characterizing structure and interactions of membrane proteins in living cells.

Graphical Abstract

*Corresponding Author rwvachet@chem.umass.edu; Phone: (413) 545-2733 (R.W.V.).

Eric M. Graban is an employee of QuarryBio Inc, which is commercializing DEPC CL-MS methods to characterize the higher order structure of protein therapeutics.

ASSOCIATED CONTENT

Supporting Information

Additional information, including additional experimental methods, a cartoon representation of mTNFα structure when attached to the cell membrane, DEPC modification percentages for residues in mTNFα in complex with adalimumab, representative structural changes to mTNFα residues upon adalimumab binding, DEPC modification percentages for residues in mTNFα in complex with golimumab, representative structural changes to mTNFα residues upon golimumab binding, DEPC modification percentages for residues in mTNFα in complex with infliximab, representative structural changes to mTNFα residues upon infliximab binding, and supplemental references. The Supporting Information is available free of charge on the ACS Publications website at DOI:

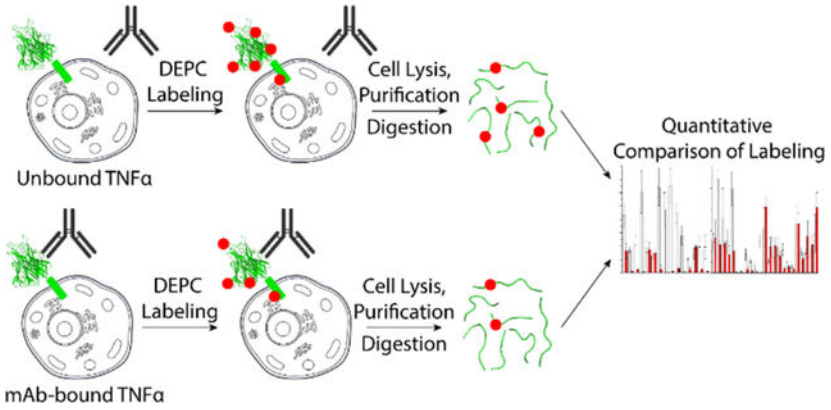

Introduction

Membrane proteins account for about 25% of the human proteome and carry out numerous functions ranging from cell signaling to cell-cell adhesion. Some viruses, including coronaviruses, for example, utilize membrane proteins as receptors to facilitate cellular entry.[1,2] Membrane proteins are also targets of close to 60% of the drugs approved in the US.[3,4] Despite their importance, characterizing their higher-order structures (HOS) and binding interactions is challenging when compared to water-soluble proteins as they have extensive hydrophobic domains, are often flexible, and are prone to precipitation when removed from their lipid bilayer.[5]

Analyzing membrane protein HOS usually involves studying the soluble domain alone or the full protein in an artificial membrane. Analysis of the soluble portion of a membrane protein is straightforward, but limited information is obtained, as the full context of the protein is not included. Embedding the protein into an artificial membrane,[6,7] such as a micelle, bicelle, amphipol, vesicle, or lipid nanodisc, better resembles cell membrane environments, but it does not fully account for the diversity of components that are present in real cell membranes. For instance, lipid rafts and asymmetric membrane bilayers are crucial for membrane protein function, and cytoskeletal components dictate membrane phase behavior and architecture, thus influencing membrane protein assembly and HOS.[8] Therefore, analyzing membrane proteins in cells, not just artificial membranes, is important.

Membrane protein structures are commonly characterized by X-ray crystallography, nuclear magnetic resonance (NMR), cryo-electron microscopy (cryo-EM), and various fluorescence spectroscopies. X-ray crystallography is not applicable to membrane proteins in cells, and NMR is challenging to apply in such settings. Cyro-EM holds great promise for membrane protein HOS analysis, although its resolution for intact cell studies is currently somewhat limited.[9–11] Several novel fluorescence techniques have been developed recently to study membrane protein oligomerization in live cells, but they are unable to provide domain-specific, much less residue-specific, structural information.[12]

Mass spectrometry (MS) has emerged as a powerful tool for studying protein HOS and interactions and is beginning to be applied to membrane proteins.[13–16] Native

MS measurements of membrane proteins, which are typically solubilized in artificial membrane systems, enable the characterization of protein complex stoichiometries, ligand-binding affinities, and ligand-induced conformational changes.[17] More resolved structural information about membrane proteins can be gathered from labeling methods such as hydrogen-deuterium exchange,[18–21] chemical cross linking (XL),[22,23] and covalent labeling (or footprinting).[24,25] These approaches encode structural information into the mass of the protein that is then 'read-out' after proteolytic digestion and LC-MS/MS analyses.

Chemical XL and covalent labeling (CL) are intriguing methods as they have the potential to provide HOS information for membrane proteins in live cells. In both methods, HOS information is encoded via the formation of covalent bonds that survive the many steps (i.e. cell lysis, extraction, digestion, separation, MS/MS) needed to analyze proteins by MS. XL-MS on intact cells has been applied to study protein interaction networks in bacteria, yeast, and mammalian cells,[26–28] although few XL-MS studies have focused on membrane proteins in live cells, because of the challenges associated with their MS detection.

CL-MS methods have recently been applied for structural characterization in live cells due to the technique's inherent simplicity and structural resolution. CL reagents can react with a wide variety of residue types, and the resulting MS and MS/MS data are simpler to interpret and use to obtain residue-level structural resolution. Fast photochemical oxidation of proteins (FPOP) has been most commonly applied to study proteins in living cells.[29–31] In FPOP, cells are incubated with hydrogen peroxide that upon irradiation with a UV laser produces hydroxyl radicals that react with solvent-accessible amino acid side chains. This approach can lead to the oxidation of any cellular proteins because hydrogen peroxide readily crosses the cell membrane. Protein oxidation includes membrane proteins, but because these proteins are underrepresented in most proteomic approaches, they have not been a focus of FPOP studies. Residue-specific labeling reagents, such as N-ethylmaleimide for Cys residues and the combination of 1-ethyl-3-(3-(dimethylamino)propyl)carbodiimide (EDC) and glycine ethyl ester (GEE) for Asp and Glu residues, have been explored to study membrane proteins in living cells,[32,33] but these reagents and approaches provide limited structural information.

Given the potential of CL-MS to provide membrane protein HOS and binding information, we have begun to investigate diethylpyrocarbonate (DEPC) as a reagent for live cell studies. DEPC can modify a range of nucleophilic residues, including His, Lys, Tyr, Ser, Thr, Cys, and the N-terminus, thereby providing excellent structural coverage. Previous work has shown the potential of this reagent to study membrane associated proteins in artificial membrane systems,[34–36] but the applicability of this reagent for studying membrane protein structure and interactions in living cells has not been demonstrated to our knowledge. Here, we describe investigations of whether DEPC-based CL-MS can successfully identify binding sites on a transmembrane protein in living cells. As a testbed, we study the binding of three monoclonal antibodies (mAbs) to membrane-bound tumor necrosis factor α (mTNFα) in HEK293T cells. Each of the three mAbs recognize a slightly different epitope on TNFα,[37] providing a robust test of the ability of DEPC CL-MS to obtain binding information for membrane proteins in cells. Our results show that mTNFα residues that are buried upon mAb binding undergo significant decreases in labeling, as expected. In addition,

we find some residues distant from the epitope also undergo changes in labeling extents that provide new insight into HOS changes associated with mAb binding. Altogether, our results show DEPC-based CL-MS is a promising approach for studying membrane protein binding in living cells.

Materials and Methods

Materials

Golimumab formulation (Simponi, lot no. HJSV01, Janssen), infliximab formulation (Remicade, lot no. HIL49016P1, Janssen), adalimumab formulation (Humira, lot no. 1088193, Abbvie), and rituximab formulation (Rituxan, lot no. 3209283, Genentech) were purchased from Myoderm.

Diethylpyrocarbonate (DEPC), dimethyl sulfoxide (DMSO), Tris, iodoacetamide, sequencing-grade trypsin, and Protease Inhibitor Tablets were purchased from Sigma-Aldrich. LC-MS grade formic acid, LC-MS grade acetonitrile, LC-MS grade water, CaptureSelect beads, Bond-Breaker tris(2-carboxyethyl)phosphine (TCEP) solution neutral pH, Halt Protease & Phosphatase Single-Use Inhibitor Cocktail, DMEM high glucose (4 g/L) media, Opti-MEM, Lipofectamine 3000 transfection reagent, phosphate-buffered saline (PBS), benzonuclease, dodecyl-β-D-maltose (DDM), cholesteryl hemisuccinate tris salt (CHS), and fetal bovine serum (FBS) were purchased from ThermoFisher Scientific.

Protein Deglycosylation Mix II and the restriction enzymes KPN1 and XBA1 were purchased from New England Biolabs. HEK293T cells purchased from ATCC. mTNFα primers were purchased from IDT-DNA. BigDye Terminator v. 3.1 Cycle Sequencing Kit was purchased from Applied Biosystems.

mTNFα Plasmid Transfection

HEK293T cells were cultured in DMEM high glucose media (4 g/L, ThermoFisher) supplemented with 10% FBS. The cells were transfected in T-75 flasks at 70% confluence using DNA encoding membrane-bound TNFα (mTNFα) with a four-residue C-terminal purification tag, EPEA, which was created by using polymerase chain reaction (PCR). The details of this procedure can be found in the Supporting Information (SI).

Protein expression, extraction efficiency, and tracking of mTNFα through purification was verified by western blot analysis using the Invitrogen Bolt™ system (Thermo Fisher Scientific), as described in the SI.

DEPC Labeling and Cell Lysis

Each experimental replicate represents one T-75 flask prepared as described in the previous section. Experiments were initiated 24 h after transfection. The cells were washed twice with cold PBS, discarded, then exposed to 1 mL of PBS supplemented with 150 μg mAb and incubated for 5 min at room temperature to ensure binding saturation. The PBS was removed, supplemented with 20 μL of 1 M DEPC pre-diluted in dimethyl sulfoxide (DMSO), and then immediately returned to the flask to initiate labeling. The final DEPC concentration in the cell media was 20 mM. The 1 M stock of DEPC in DMSO was

prepared immediately before use. The cells were reacted with DEPC for 5 min at room temperature. The DEPC reaction was quenched by addition of 50 μL of 1 M Tris pH 8 directly to the wells. 10 μL of 500 mM iodoacetamide in 1 M Tris pH 8 was then added to the plate to alkylate any free cysteines which may be present within the cells to avoid DEPC scrambling.[38]

To lyse the cells, a solution of MS-compatible detergents were used. This procedure is described in the SI.

Purification and Digestion of mTNFα from Cell Lysate

CaptureSelect™ beads were used with gravity filtration columns for mTNFα enrichment, as described in the SI.

Proteolytic processing of samples started with a pre-digest using 1 μg of Lys-C and incubated for 1 h at 37°C. Next, 5 μL of 0.5 M TCEP (Bond-Breaker) was added to each sample, mixed, and immediately followed by addition of 10 μL of 500 mM iodoacetamide in 1 M Tris pH 8.0. The addition of excess reducing agent immediately followed by alkylating agent was done this way to minimize label scrambling. Samples were then incubated for 20 minutes at 37 °C. After alkylation, the samples were then diluted to 150 μL using 25 mM Tris pH 8 and supplemented with 2 μL of Protein Deglycosylation Mix II and incubated for 90 minutes at 37°C. Trypsin was reconstituted in 25 mM Tris pH 8 to 1 mg/mL, and 6 μL of this trypsin solution was added to each sample. The samples were then digested for 3 hours at 37 °C before inactivation by addition of 7.5 μL of 10% formic acid. Digests were then flash-frozen in liquid N_2 until LC-MS/MS analysis.

LC-MS/MS Analysis

Online LC-MS/MS analysis was performed using a Dionex Ultimate 3000 (Thermo Scientific, Tewksbury, MA). The flow rate was 10 μL/min. Peptides were eluted on a ZORBAX 300SB-C18 MicroBore RR column (1.0 × 150 mm, 3.5 μm particle size, Agilent, Wilmington, DE) with LC-MS grade water and 0.1% formic acid as solvent A and LC-MS grade acetonitrile (ACN) with 0.1% formic acid as solvent B. A linear gradient from 5 to 35% over 85 min with a final wash at 80% B for 5 min was used. Mass spectra were acquired using a Thermo Scientific Orbitrap LTQ-Elite mass spectrometer with an electrospray ionization source. The electrospray ionization source was used in the positive mode with a needle voltage of 5000 V. Tandem mass spectra were generated using data-dependent acquisition with a CID collision energy of 35. Following an MS1 scan the 15 most intense ions were selected for rapid MS/MS with dynamic exclusion of repeat scans for 180 sec. A custom software pipeline designed for DEPC-CL/MS was used to analyze the LC-MS/MS spectra, as described in the SI.

Results and Discussion

DEPC reaction optimization and membrane protein purification

Minimizing perturbations to cells is important in these studies to ensure accurate protein binding information. DEPC has moderate solubility in water (~40 mM) so stock solutions

must be prepared in an organic solvent, with ACN being commonly used at <2% v/v to avoid protein structural pertubations.[15,40] However, adding even low percentages of ACN caused rapid cell detachment. As an alternative, DMSO at 1.7% v/v was chosen as a solvent as it did not cause cell detachment during the labeling reaction. DMSO can disrupt cell membranes, but not at the concentrations used here.[41] Furthermore, experiments with the CellTiter-Glo® assay indicate no significant change in cell viability under the labeling conditions used (Figure S1).

Typical DEPC CL-MS experiments involve comparing the labeling of free and bound protein (Figure 1). In-cell labeling experiments of TNFα-mAb complexes require additional considerations because the mAb, the cell media, and the cells themselves can influence DEPC reactivity. In previous work, we showed that a non-binding protein was necessary as a control to account for the greater number of labelable sites available with a mAb present.[42] Rituximab was chosen for this non-binding control in experiments described here because it does not bind to TNFα and has a comparable number of labelable sites to the mAbs that do bind (see Table S1).

Because membrane proteins like mTNFα can be difficult to detect in the presence of more abundant cytosolic proteins, mTNFα was expressed with an EPEA C-terminal affinity tag to enable enrichment of the protein. EPEA was chosen as the affinity tag because it has no DEPC-labelable residues, so purification of DEPC-labeled and unlabeled mTNFα should be identical.

Upon applying these optimized conditions and using the affinity tag, we were able to obtain good structural coverage of mTNFα in cells from the DEPC labeling experiments. Tryptic digestion of purified mTNFα resulted in approximately 85% overall sequence coverage with 99% of the extracellular region and 82% of the intracellular region being detected (Figure S2). mTNFα is a 233-residue transmembrane protein consisting of four His, eight Lys, 20 Ser, 10 Thr, and seven Tyr residues, for a total of 49 labelable sites (Figure S3). We observed labeling at 30 of these sites, accounting for approximately 60% of the labelable sites when the protein was reacted in cells with 20 mM DEPC for 5 min. The labeling was primarily located on the extracellular domain, but two Lys residues on the intracellular domain were also labeled. This extent of labeling is comparable to what we observed in previous work with soluble TNFα (sTNFα) in free solution.[42] Although, it should be noted that higher DEPC concentrations were needed in the present studies due to the greater number of molecules that could react or interact with DEPC in cell culture.

To test the ability of DEPC CL-MS to provide correct protein binding information in cell culture, three therapeutic mAbs, each recognizing slightly different epitopes on TNFα, were studied.[37,43,44] For the purposes of this work, the epitope residues are defined as (i) those with at least one non-hydrogen atom within 5 Å of the bound mAb and/or (ii) those that are buried upon complexation with the mAb (see the Supporting Methods for a more detailed description). A caveat is that the epitopes for these mAbs are based on crystal structures of sTNFα (i.e. most of the extracellular domain of mTNFα) in complex with the antigen-binding (Fab) domains of the mAbs, whereas in our experiments the full-length

mAbs were added in culture to cells containing membrane-inserted TNFα, which includes its full extracellular, transmembrane and intracellular domains.

mTNFα in complex with adalimumab

Adalimumab has the largest epitope of the three mAbs studied, comprising two protomers of the TNFα trimer (Figure 2A). The epitope has residues in the A and D β-strands and in the A-A', D-E, E-F, and G-H loops (Figure 2B).[37] There are 16 residues in the epitope region that can be labeled, and 13 of them are modified by DEPC in the presence of rituximab (i.e. non-binding control) or adalimumab. Nine of these residues undergo significant changes in labeling upon comparing the rituximab control and adalimumab (Figure 2C and Table S2). Seven of these nine residues, including Lys140, Ser146, Thr147, Lys165, Ser170, Ser174, and Lys187, decrease in labeling because of burial upon adalimumab binding to mTNFα (Figure 2D). His148, Thr152, His153, and Lys173 do not significantly change in labeling, perhaps because the adalimumab epitope in mTNFα is slightly different than in sTNFα. Such a difference would be consistent with the lower dissociation constant (K_d) that has been measured for mTNFα as compared to sTNFα.[45]

Two of the epitope residues, Tyr216 and Tyr190, increase in labeling (Figure 2E). Tyr216 is located on the edge of where adalimumab binds the mTNFα trimer. The hydroxyl group of Tyr216 is comparably exposed in bound and unbound mTNFα and is not buried by bound adalimumab. Its increased labeling can be explained by the increase in hydrophobic microenvironment introduced by the binding of adalimumab. It has been shown previously that Ser, Thr, and Tyr residues can undergo an increase in DEPC labeling when they go from exposed to a more hydrophobic microenvironment, which increases the reactivity of these residues through an increased local concentration of DEPC.[46,47] This phenomenon is particular to Ser, Thr, and Tyr residues because of their weak nucleophilicity compared to Lys and His. The increased labeling of Tyr190 is more difficult to explain because Tyr190 should be buried upon binding to adalimumab. Perhaps the epitope region of mTNFα for adalimumab is slightly different than in sTNFα. This same Tyr residue (Tyr115 in sTNFα) undergoes a slight decrease in DEPC labeling when studying the adalimumab-sTNFα complex in previous work.[42] Tyr190 is at the end of a β-strand near the TNFα trimer interface, and adalimumab is known to stabilize the TNFα trimer in the soluble version of the protein.[48] Perhaps adalimumab binding to the membrane-bound version of TNFα influences the trimer interface in a different manner, thereby changing the microenvironment around Tyr190.

In addition to the 13 labeled residues in the epitope, there are 17 non-epitope residues that are labeled, seven of which significantly change in labeling (Figure 2C). Four of these seven residues decrease in labeling: Ser84, Thr180, Tyr194, and Lys203. Thr180 is approximately 10 Å from the nearest adalimumab contact, and its decrease in labeling could be attributed to a change in its microenvironment upon adalimumab binding as DEPC labeling of Thr, Ser, and Tyr residues is very sensitive to changes in microenvironment (Figure S4A).[46] Tyr194 is located at the TNFα trimer interface. Adalimumab stabilizes the sTNFα trimer, and in previous DEPC CL-MS studies of sTNFα, we found that this same Tyr residue undergoes a change in labeling upon adalimumab binding.[42,48] It is possible

that the binding of adalimumab affects the way the mTNFα trimer packs together, changing the microenvironment of Tyr194 (Figure S4B). Ser84 and Lys203 are both distant from the epitope and trimer interface; however, they are near the membrane-associated end of the trimer (Figure S4C) that undergoes a conformational change upon binding to the TNFα receptor on nearby cells. This conformational change occurs in the linker that connects the transmembrane and extracellular domains, and results in the protein compacting up against the cell membrane.[49] While it is unknown if this compaction of the linker occurs in the absence of TNFα receptors, because adalimumab competitively inhibits the binding of TNFα to the TNFα receptor, it is likely that a similar conformational change occurs upon adalimumab binding, explaining why Ser84 and Lys203 decrease in labeling.[37]

Three non-epitope residues increase in labeling: Ser161, Tyr162, and Ser208. The increases observed for all three residues might be explained by their proximity to adalimumab upon binding, which creates a more hydrophobic microenvironment (Figure S4D). A comparable effect was shown in previous studies with sTNFα, where Ser, Thr, and Tyr residues on the periphery of the epitope region increased in labeling as a result of a more hydrophobic microenvironment.[42] Overall, despite some epitope residues not undergoing the expected changes in labeling, the DEPC CL-MS results are largely consistent with the structure of the TNFα-adalimumab complex in free solution, suggesting that DEPC CL-MS is valuable for studying membrane protein interactions in live cells. Moreover, the labeling results for the non-epitope residues provide new insight into how the rest of the protein likely restructures upon binding to adalimumab.

mTNFα in complex with golimumab

Golimumab has the smallest epitope of the three mAbs studied, comprising residues in the A-A', C-D, E-F, and G-H loops (Figure 3A).[44] Unlike adalimumab, golimumab binds only a single protomer in the TNFα trimer. There are six labelable residues in the epitope, all of which are labeled in the control or in the presence of golimumab. Two of the six residues undergo significant decreases in labeling because of burial on golimumab binding: Thr147 and Thr180 (Figure 3B). Ser146 and Tyr216 also did not significantly change in labeling. The lack of labeling changes for Ser146 and Tyr216 are perplexing as they are buried to similar extents as Thr147 in the sTNFα-golimumab complex. For reasons that are not clear, there are fewer overall labeling changes in the golimumab experiments than observed in the adalimumab and infliximab experiments (see below). In previous DEPC CL-MS work with soluble TNFα, 17 total significant changes were observed when golimumab was bound, 17 when adalimumab was bound, and 13 when infliximab was bound.[42] However, in cell-based experiments described here, there are only nine significant changes when golimumab is bound and 16 and 19 for adalimumab and infliximab, respectively. This discrepancy may suggest that golimumab is not binding mTNFα in the cells to the same extent as adalimumab or infliximab, hindering us from better mapping the epitope.

There are 24 residues outside of the epitope that are labeled, seven of which undergo significant changes in labeling (Figure 3C). Four of these seven residues decrease in labeling: Ser174, Tyr194, Lys203, and Ser208. Ser174 and Tyr194 are near the TNFα trimer interface, so it is possible that changes to the way the trimer packs together upon

golimumab binding causes these decreases, as was seen with adalimumab (Figure S5A). Decreased labeling of Lys203 might occur for the same reason that it does in adalimumab via compaction of this linker region of mTNFα against the cell membrane upon golimumab binding (Figure S4C). Curiously, however, Ser84 does not undergo a decrease in labeling as it did with adalimumab. Ser208 decreased labeling might be explained by an uncharacterized allosteric structural change upon antibody binding, as this residue is distant from the epitope, not part of the trimer interface, and not close enough to the linker to compact against the cell membrane (Figure S5B).

The remaining three of the seven significant changes are increases in labeling: His148, Ser161, and Tyr190. His148 is close to a neighboring TNFα protomer (Figure S5C), so it is possible that golimumab binding causes this residue to re-orient in a way that increases its solvent accessibility and reactivity with DEPC. Ser161 is distant from the epitope, trimer interface, and linker region, so its increase in labeling is more challenging to explain. It is possible that Ser161 undergoes a change in microenvironment because of a conformational change of the D-E loop upon golimumab binding (Figure S5D), as was observed in DEPC labeling studies of soluble TNFα.[42] Tyr190 is located on the edge of the epitope, and the proximity of Tyr53, Gly55, and Ser56 from golimumab (Figure S5E) likely create a more hydrophobic microenvironment that accounts for the increased labeling of this residue. Overall, the DEPC labeling results for mTNFα bound to golimumab are not as clearly indicative of the epitope as was observed with adalimumab, but the results are consistent with other structural features.

mTNFα in complex with infliximab

The infliximab epitope is made up of residues in the C-D and E-F loops as well as residues in the C and D β-strands (Figure 4A).[43] Similar to golimumab, infliximab only binds one protomer of the mTNFα trimer. There are seven labelable residues in the epitope, all of which are labeled by DEPC in the control or in the presence of infliximab. Six of the seven epitope residues undergo significant decreases in labeling because of burial upon infliximab binding: Ser146, Thr147, His148, Thr152, Thr180, and Lys187 (Figure 4B). Tyr216 did not undergo any significant change in labeling, perhaps because the infliximab epitope in mTNFα is slightly different than in sTNFα.

Outside of the epitope, 22 residues are labeled, of which 13 significantly change in labeling (Figure 4C and Table S4). Ser70, His90, Tyr134, Lys140, Thr164, Lys165, Ser174, Tyr194, Lys203, and Ser208 decrease in labeling. Ser70 is part of the extracellular domain of mTNFα but is not present in crystal structures of sTNFα because it is part of the mTNFα sequence that is cleaved off by TNFα converting enzyme to produce the soluble form. Therefore, there is no structural information available to predict what happens with this residue. Similar to the decrease observed for Ser84 and Lys203 upon adalimumab binding, compaction of the mTNFα trimer against the cell membrane upon binding to infliximab could bury this residue. The same potential phenomenon explains the decrease in Lys203 labeling too (Figure S4C).

Decreased labeling of His90, Tyr134, Ser174, and Tyr194 may be explained by their presence at the TNFα trimer interface (Figure S6A). Like adalimumab, infliximab stabilizes

the sTNFα trimer in solution, although to a lower extent, so it is likely that infliximab binding changes the microenvironment of these interfacial residues, causing a change in DEPC reactivity.[48] Lys140 is approximately 6 Å from infliximab, so it is not part of the infliximab epitope by our definition; however, upon infliximab binding, the side chain of Lys140 is partially blocked (Figure S6B), explaining its decrease in labeling. Thr164, Lys165, and Ser208 also decrease in labeling. These residues are distant from the epitope, not part of the trimer interface, nor are they in the vicinity of the linker region such that they might approach the cell membrane upon infliximab binding. All three residues are close in 3D space (Figure S6C), though, so it is possible that infliximab binding causes some uncharacterized allosteric change in this region of mTNFα that results in labeling changes.

Three residues are observed to increase in labeling upon infliximab binding: Tyr162, Lys173, and Tyr190. In free and complexed sTNFα, Tyr162 is exposed, but perhaps the same uncharacterized structural change that influences the reactivity of nearby Thr164, Lys165, and Ser208 also changes the microenvironment and thus DEPC reactivity of Tyr162. Lys173 is located at the trimer interface and forms a salt bridge with Glu191. It is possible that infliximab binding disrupts this salt bridge, enabling Lys173 to react more extensively with DEPC (Figure S6D). The increased labeling of Tyr190 is most likely explained by its position at the periphery of the epitope. Phe and Val residues on nearby infliximab (Figure S6E) provide a more hydrophobic microenvironment that increases Tyr190 labeling. Overall, like the adalimumab results, the DEPC CL-MS results with infliximab are largely consistent with the structure of the TNFα complex, indicating that DEPC CL-MS is valuable for studying membrane protein interactions in live cells.

Conclusions

We demonstrate here that DEPC CL-MS can successfully provide epitope information for membrane proteins in living cells. Using therapeutic mAbs that bind mTNFα, we find residues that are buried in the epitope upon binding to the mAbs adalimumab and infliximab generally decrease in DEPC labeling extent. In addition, residues on the periphery of the epitope – particularly Ser, Thr, and Tyr residues – increase in labeling upon binding to these two mAbs because of a more hydrophobic microenvironment that is created by the bound mAb. In effect, a “bull’s eye” is created around the epitope with completely buried residues protected from labeling and partially buried Ser, Thr, and Tyr residues undergoing an increase in labeling. In a few instances, residues known to be in the epitope of the soluble version of TNFα (i.e. sTNFα) did not significantly change in labeling extent, suggesting that the epitopes on mTNFα may be slightly different. Away from the epitope, we observe changes in labeling upon mAb binding that suggest changes to the packing of the mTNFα homotrimer, compaction of the protein against the cell membrane, and/or previously uncharacterized allosteric changes upon mAb binding. It is important to note that the experiments with golimumab, which do not as clearly indicate the epitope as with adalimumab and infliximab, suggest that sufficient antibody binding to the membrane protein is necessary to observe sufficient changes in DEPC labeling.

Overall, DEPC CL-MS seems to have excellent potential for studying membrane protein binding in living cells, offering a new means of characterizing the structure and interactions

of these difficult to study protein systems. While the current work investigates a protein that has been expressed with a tag to facilitate its enrichment and detection, endogenous membrane proteins could be investigated too as long as enough labeled tryptic fragments are detected for these proteins. One could even envision using a labeling reagent that contains an enrichment handle itself to further facilitate detection.

Supplementary Material

Refer to Web version on PubMed Central for supplementary material.

Acknowledgements

This work was supported by the National Institutes of Health (NIH) under grants R01 GM075092, R35 GM145272, and R43 GM116211. We also acknowledge Dr. John Hale for his advice on data analysis.

Data availability

The raw mass spectrometric data can be accessed in Massive (MassIVE MSV000091232).

References:

(1). Shang J; Wan Y; Luo C; Ye G; Geng Q; Auerbach A; Li F Cell Entry Mechanisms of SARS-CoV-2. Proc. Natl. Acad. Sci. U. S. A. 2020, 117 (21), 11727–11734. [PubMed: 32376634]

(2). Marsh M; Helenius A Virus Entry: Open Sesame. Cell 2006, 124 (4), 729–740. [PubMed: 16497584]

(3). Overington JP; Al-Lazikani B; Hopkins AL How Many Drug Targets Are There? Nat. Rev. Drug Discov. 2006, 5 (12), 993–996. [PubMed: 17139284]

(4). Yin H; Flynn AD Drugging Membrane Protein Interactions. Annu. Rev. Biomed. Eng. 2016, 18, 51–76. [PubMed: 26863923]

(5). Carpenter EP; Beis K; Cameron AD; Iwata S Overcoming the Challenges of Membrane Protein Crystallography. Curr. Opin. Struct. Biol. 2008, 18 (5), 581–586. [PubMed: 18674618]

(6). Kang CB; Li Q Solution NMR Study of Integral Membrane Proteins. Curr. Opin. Chem. Biol. 2011, 15 (4), 560–569. [PubMed: 21684799]

(7). Majeed S; Ahmad AB; Sehar U; Georgieva ER Lipid Membrane Mimetics in Functional and Structural Studies of Integral Membrane Proteins. Membranes (Basel). 2021, 11 (9), 1–29.

(8). Eeman M; Deleu M From Biological Membranes to Biomimetic Model Membranes. Biotechnol. Agron. Soc. Environ. 2010, 14 (4), 719–736.

(9). Thonghin N; Kargas V; Clews J; Ford RC Cryo-Electron Microscopy of Membrane Proteins. Methods 2018, 147, 176–186. [PubMed: 29702228]

(10). Chen W; Kudryashev M Structure of RyR1 in Native Membranes. EMBO Rep. 2020, 21 (5), 1–11.

(11). Yao X; Fan X; Yan N Cryo-EM Analysis of a Membrane Protein Embedded in the Liposome. Proc. Natl. Acad. Sci. U. S. A. 2020, 117 (31), 18497–18503. [PubMed: 32680969]

(12). Christie S; Shi X; Smith AW Resolving Membrane Protein-Protein Interactions in Live Cells with Pulsed Interleaved Excitation Fluorescence Cross-Correlation Spectroscopy. Acc. Chem. Res. 2020, 53 (4), 792–799. [PubMed: 32227891]

(13). Konermann L; Pan J; Liu YH Hydrogen Exchange Mass Spectrometry for Studying Protein Structure and Dynamics. Chem. Soc. Rev. 2011, 40 (3), 1224–1234. [PubMed: 21173980]

(14). Yu C; Huang L Cross-Linking Mass Spectrometry: An Emerging Technology for Interactomics and Structural Biology. Anal. Chem. 2018, 90 (1), 144–165. [PubMed: 29160693]

(15). Limpikirati P; Liu T; Vachet RW Covalent Labeling-Mass Spectrometry with Non-Specific Reagents for Studying Protein Structure and Interactions. Methods 2018, 144, 79–93. [PubMed: 29630925]

(16). Liu XR; Zhang MM; Gross ML Mass Spectrometry-Based Protein Footprinting for Higher-Order Structure Analysis: Fundamentals and Applications. Chem. Rev. 2020, 120 (10), 4355–4454. [PubMed: 32319757]

(17). Calabrese AN; Radford SE Mass Spectrometry-Enabled Structural Biology of Membrane Proteins. Methods 2018, 147, 187–205. [PubMed: 29510247]

(18). Hebling CM; Morgan CR; Stafford DW; Jorgenson JW; Rand KD; Engen JR Conformational Analysis of Membrane Proteins in Phospholipid Bilayer Nanodiscs by Hydrogen Exchange Mass Spectrometry. Anal. Chem. 2010, 82 (13), 5415–5419. [PubMed: 20518534]

(19). Vahidi S; Bi Y; Dunn SD; Konermann L Load-Dependent Destabilization of the γ-Rotor Shaft in FOF1 ATP Synthase Revealed by Hydrogen/Deuterium-Exchange Mass Spectrometry. Proc. Natl. Acad. Sci. U. S. A. 2016, 113 (9), 2412–2417. [PubMed: 26884184]

(20). Reading E; Hall Z; Martens C; Haghighi T; Findlay H; Ahdash Z; Politis A; Booth PJ Interrogating Membrane Protein Conformational Dynamics within Native Lipid Compositions. Angew. Chemie - Int. Ed 2017, 56 (49), 15654–15657.

(21). Martens C; Politis A A Glimpse into the Molecular Mechanism of Integral Membrane Proteins through Hydrogen–Deuterium Exchange Mass Spectrometry. Protein Sci. 2020, 29 (6), 1285–1301. [PubMed: 32170968]

(22). Liu H; Zhang H; Niedzwiedzki DM; Prado M; He G; Gross ML; Blankenship RE Phycobilisomes Supply Excitations to Both Photosystems in a Megacomplex in Cyanobacteria. Science (80-.). 2013, 342, 1104–1107.

(23). Komolov KE; Du Y; Duc NM; Betz RM; Rodrigues JPGLM; Leib RD; Patra D; Skiniotis G; Adams CM; Dror RO; Chung KY; Kobilka BK; Benovic JL Structural and Functional Analysis of a B2-Adrenergic Receptor Complex with GRK5. Cell 2017, 169 (3), 407–421.e16. [PubMed: 28431242]

(24). Pan Y; Konermann L Membrane Protein Structural Insights from Chemical Labeling and Mass Spectrometry. Analyst 2010, 135 (6), 1191–1200. [PubMed: 20498872]

(25). Pan X; Vachet RW Membrane Protein Structures and Interactions From Covalent Labeling Coupled With Mass Spectrometry. Mass Spectrom. Rev. 2022, 41 (1), 51–69. [PubMed: 33145813]

(26). Zhang H; Tang X; Munske GR; Tolic N; Anderson GA; Bruce JE Identification of Protein-Protein Interactions and Topologies in Living Cells with Chemical Cross-Linking and Mass Spectrometry. Mol. Cell. Proteomics 2009, 8 (3), 409–420. [PubMed: 18936057]

(27). Yang B; Wu YJ; Zhu M; Fan SB; Lin J; Zhang K; Li S; Chi H; Li YX; Chen HF; Luo SK; Ding YH; Wang LH; Hao Z; Xiu LY; Chen S; Ye K; He SM; Dong MQ Identification of Cross-Linked Peptides from Complex Samples. Nat. Methods 2012, 9 (9), 904–906. [PubMed: 22772728]

(28). Shi Y; Pellarin R; Fridy PC; Fernandez-Martinez J; Thompson MK; Li Y; Wang QJ; Sali A; Rout MP; Chait BT A Strategy for Dissecting the Architectures of Native Macromolecular Assemblies. Nat. Methods 2015, 12 (12), 1135–1138. [PubMed: 26436480]

(29). Espino JA; Mali VS; Jones LM In Cell Footprinting Coupled with Mass Spectrometry for the Structural Analysis of Proteins in Live Cells. Anal. Chem. 2015, 87 (15), 7971–7978. [PubMed: 26146849]

(30). Espino JA; Jones LM Illuminating Biological Interactions with in Vivo Protein Footprinting. Anal. Chem. 2019, 91 (10), 6577–6584. [PubMed: 31025855]

(31). Espino JA; King CD; Jones LM; Robinson RAS In Vivo Fast Photochemical Oxidation of Proteins Using Enhanced Multiplexing Proteomics. Anal. Chem. 2020, 92 (11), 7596–7603. [PubMed: 32383586]

(32). Shen G; Li S; Cui W; Liu S; Yang Y; Gross M; Li W Membrane Protein Structure in Live Cells: Methodology for Studying Drug Interaction by Mass Spectrometry-Based Footprinting. Biochemistry 2018, 57 (3), 286–294. [PubMed: 29192498]

(33). Müller A; Langó T; Turiák L; Ács A; Várady G; Kucsma N; Drahos L; Tusnády GE Covalently Modified Carboxyl Side Chains on Cell Surface Leads to a Novel Method toward Topology Analysis of Transmembrane Proteins. Sci. Rep. 2019, 9 (1), 1–11. [PubMed: 30626917]

(34). Schmidt C; Macpherson JA; Lau AM; Tan KW; Fraternali F; Politis A Surface Accessibility and Dynamics of Macromolecular Assemblies Probed by Covalent Labeling Mass Spectrometry and Integrative Modeling. Anal. Chem. 2017, 89 (3), 1459–1468. [PubMed: 28208298]

(35). Guo C; Cheng M; Li W; Gross ML Diethylpyrocarbonate Footprints a Membrane Protein in Micelles. J. Am. Soc. Mass Spectrom. 2021, 32 (11), 2636–2643. [PubMed: 34664961]

(36). Zhao B; Zhuang J; Xu M; Liu T; Limpikirati P; Thayumanavan S; Vachet RW Covalent Labeling with an α,β-Unsaturated Carbonyl Scaffold for Studying Protein Structure and Interactions by Mass Spectrometry. Anal. Chem. 2020, No. 92, 6637–6644. [PubMed: 32250591]

(37). Hu S; Liang S; Guo H; Zhang D; Li H; Wang X; Yang W; Qian W; Hou S; Wang H; Guo Y; Lou Z Comparison of the Inhibition Mechanisms of Adalimumab and Infliximab in Treating Tumor Necrosis Factor α-Associated Diseases from a Molecular View. J. Biol. Chem. 2013, 288 (38), 27059–27067. [PubMed: 23943614]

(38). Zhou Y; Vachet RW Diethylpyrocarbonate Labeling for the Structural Analysis of Proteins: Label Scrambling in Solution and How to Avoid It. J. Am. Soc. Mass Spectrom. 2012, 23 (5), 899–907. [PubMed: 22351293]

(39). Borotto NB; Zhou Y; Hollingsworth SR; Hale JE; Graban EM; Vaughan RC; Vachet RW Investigating Therapeutic Protein Structure with Diethylpyrocarbonate Labeling and Mass Spectrometry. Anal. Chem. 2015, 87 (20), 10627–10634. [PubMed: 26399599]

(40). Pan X; Limpikirati P; Chen H; Liu T; Vachet RW Higher-Order Structure Influences the Kinetics of Diethylpyrocarbonate Covalent Labeling of Proteins. J. Am. Soc. Mass Spectrom. 2020, 31 (3), 658–665. [PubMed: 32013423]

(41). Lynch J; Chung JW; Huang Z; Pierce V; Saunders NS; Niu L Enhancing Transient Protein Expression in HEK-293 Cells by Briefly Exposing the Culture to DMSO. J. Neurosci. Methods 2021, 350, 109058. [PubMed: 33359979]

(42). Tremblay CY; Kirsch ZJ; Vachet RW Epitope Mapping with Diethylpyrocarbonate Covalent Labeling- Mass Spectrometry. Anal. Chem. 2022, 94, 1052–1059. [PubMed: 34932327]

(43). Liang S; Dai J; Hou S; Su L; Zhang D; Guo H; Hu S; Wang H; Rao Z; Guo Y; Lou Z Structural Basis for Treating Tumor Necrosis Factor α (TNFα)-Associated Diseases with the Therapeutic Antibody Infliximab. J. Biol. Chem. 2013, 288 (19), 13799–13807. [PubMed: 23504311]

(44). Ono M; Horita S; Sato Y; Nomura Y; Iwata S; Nomura N Structural Basis for Tumor Necrosis Factor Blockade with the Therapeutic Antibody Golimumab. Protein Sci. 2018, 27 (6), 1038–1046. [PubMed: 29575262]

(45). Kaymakcalan Z; Sakorafas P; Bose S; Scesney S; Xiong L; Karaoglu D; Salfeld J; Sasso EH Comparisons of Affinities, Avidities, and Complement Activation of Adalimumab, Infliximab, and Etanercept in Binding to Soluble and Membrane Tumor Necrosis Factor. Clin. Immunol. 2009, 131 (2), 308–316. [PubMed: 19188093]

(46). Limpikirati P; Pan X; Vachet RW Covalent Labeling with Diethylpyrocarbonate: Sensitive to the Residue Microenvironment, Providing Improved Analysis of Protein Higher Order Structure by Mass Spectrometry. Anal. Chem. 2019, 91, 8516–8523. [PubMed: 31150223]

(47). Biehn SE; Limpikirati P; Vachet RW; Lindert S Utilization of Hydrophobic Microenvironment Sensitivity in Diethylpyrocarbonate Labeling for Protein Structure Prediction. Anal. Chem. 2021, 93 (23), 8188–8195. [PubMed: 34061512]

(48). Van Schie KA; Ooijevaar-De Heer P; Dijk L; Kruithof S; Wolbink G; Rispens T Therapeutic TNF Inhibitors Can Differentially Stabilize Trimeric TNF by Inhibiting Monomer Exchange. Sci. Rep. 2016, 6, 1–10. [PubMed: 28442746]

(49). Tang P; Hung MC; Klostergaard J Human Pro-Tumor Necrosis Factor Is a Homotrimer. Biochemistry 1996, 35 (25), 8216–8225. [PubMed: 8679576]

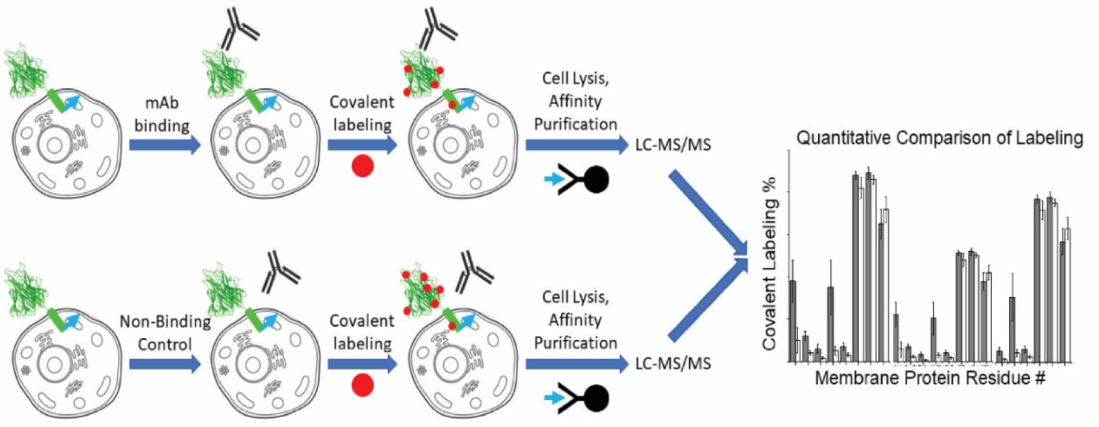

Figure 1.

Workflow for in-cell labeling of mTNFα. mTNFα expressed in HEK293T cells was incubated with a binding or non-binding mAb and then labeled by DEPC. After the DEPC reaction, the cells were lysed, and the protein was purified from the cell lysate using a C-terminal EPEA affinity tag. LC-MS/MS was then used to compare the labelling extents between the two conditions.

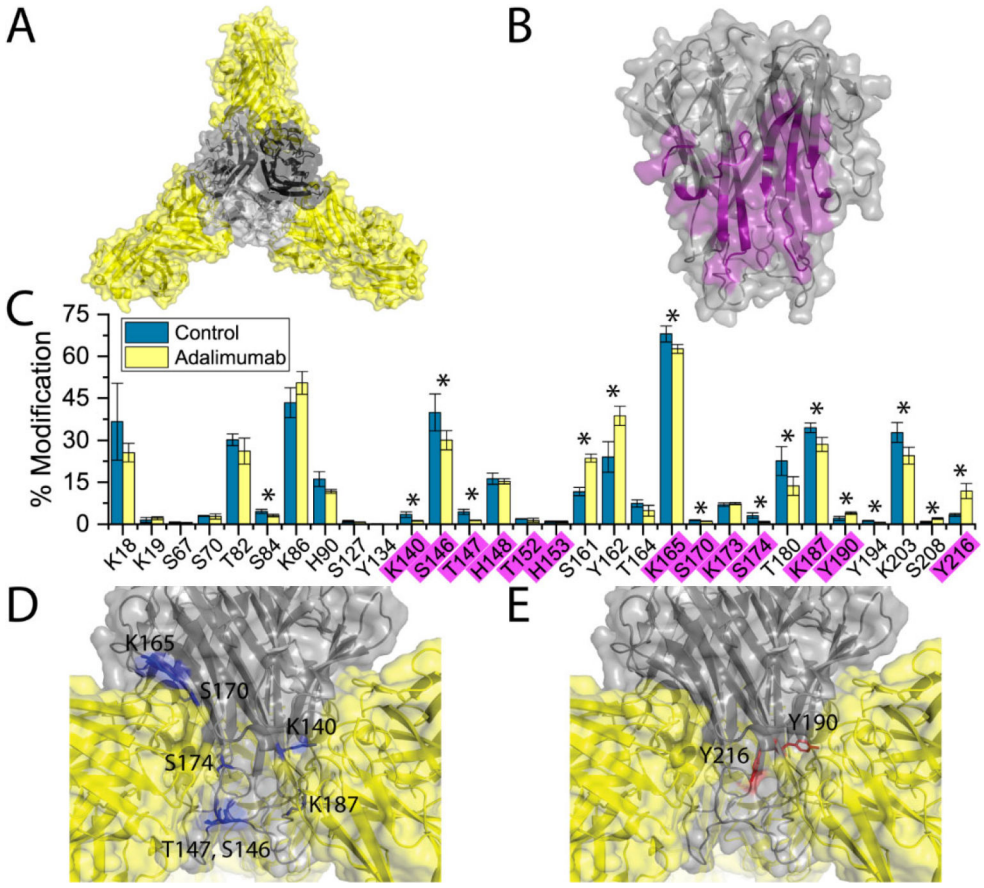

Figure 2.

Structure and DEPC labeling results of TNFα in complex with adalimumab. (A) Surface/cartoon representation of three adalimumab Fab fragments in complex with sTNFα trimer (PDB ID: 3WD5). (B) sTNFα trimer structure with epitope residues across two TNFα protomers colored in purple (PDB ID: 1TNF). (C) DEPC labeling extents for mTNFα residues with and without full-length adalimumab bound. Epitope residues are highlighted in purple and statistically significant changes in labeling at 90% confidence are marked with an asterisk. (D) Epitope residues that decrease in labeling (blue) upon adalimumab binding, mapped on the sTNFα trimer. The adalimumab Fab fragments are shown in yellow and the sTNFα trimer is shown in gray. (E) Epitope residues that increase in labeling (red) upon adalimumab binding, mapped on the sTNFα trimer.

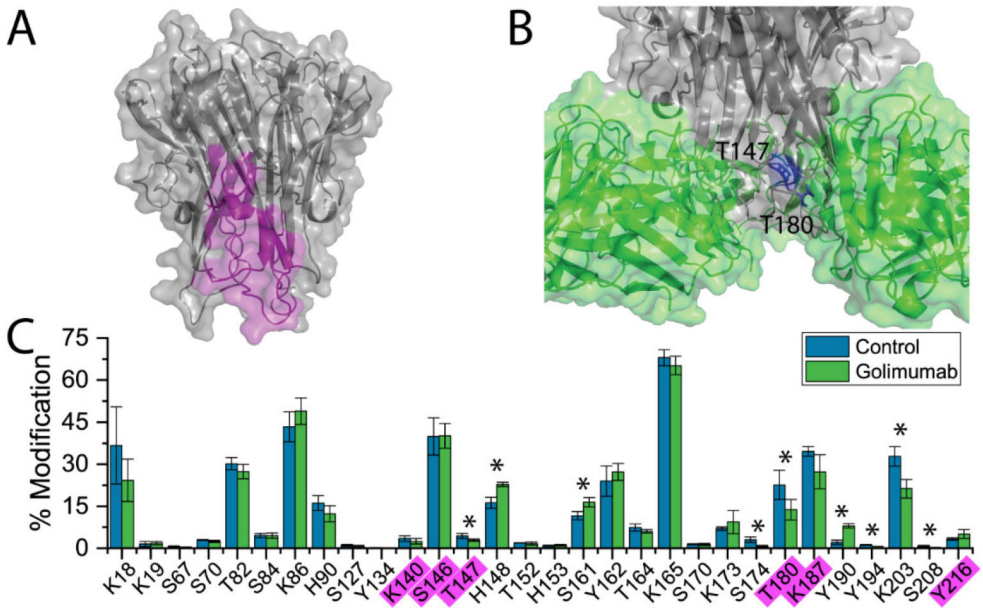

Figure 3.

Structure and DEPC labeling results of TNFα in complex with golimumab. (A) sTNFα trimer structure with epitope residues on one TNFα protomer colored in purple (PDB ID: 1TNF). (B) Epitope residues that decrease in labeling (blue) upon golimumab binding, mapped on the sTNFα trimer. The golimumab Fab fragments are shown in green and the sTNFα trimer is shown in gray (PDB ID: 5YOY). (C) DEPC labeling extents for mTNFα residues with and without full-length golimumab bound. Epitope residues are highlighted in purple and statistically significant changes in labeling at 90% confidence are marked with an asterisk.

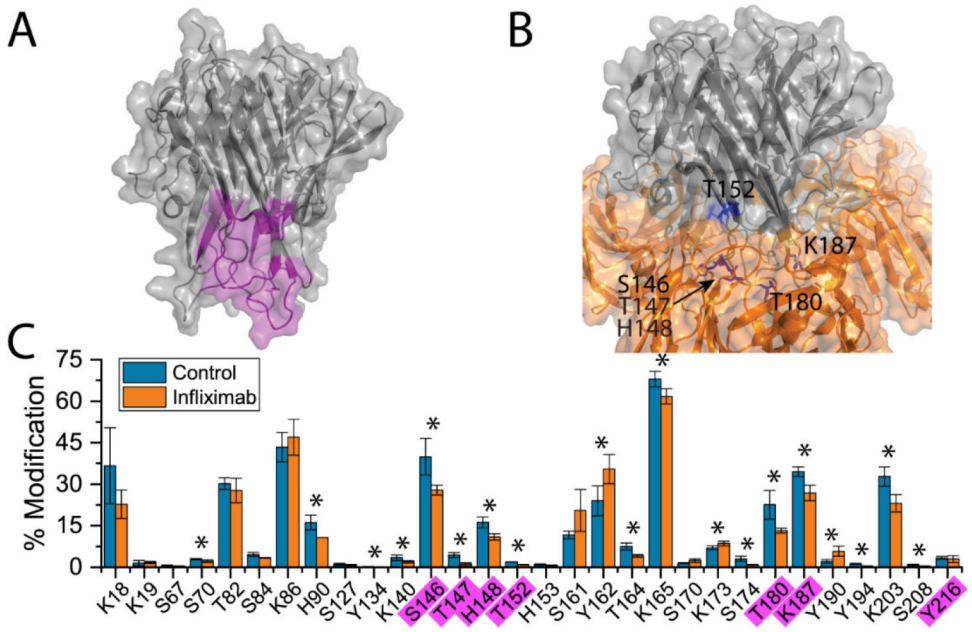

Figure 4.

Structure and DEPC labeling results of TNFα in complex with infliximab. (A) sTNFα trimer structure with epitope residues on one TNFα protomer colored in purple (PDB ID: 1TNF). (B) Epitope residues that decrease in labeling (blue) upon infliximab binding, mapped on the sTNFα trimer. The infliximab Fab fragments are shown in orange and the sTNFα trimer is shown in gray (PDB ID: 4G3Y). (C) DEPC labeling extents for mTNFα residues with and without full-length infliximab bound. Epitope residues are highlighted in purple and statistically significant changes in labeling at 90% confidence are marked with an asterisk.